Robotics and Computer Integrated Manufacturing 61 (2020) 101819

Contents lists available at ScienceDirect

Robotics and Computer Integrated Manufacturing

journal homepage: www.elsevier.com/locate/rcim

Estimating probability of human hand intrusion for speed and separation monitoring using interference theory

Eugene Kim*[a], Robin Kirschner[b], Yoji Yamada[a], Shogo Okamoto[a]

[a] Department of Mechanical Systems Engineering, Nagoya University, Furo-Cho, Chikusa-ku, Nagoya, 464-8603, Japan
[b] Department of Mechanical Engineering, Chemnitz University of Technology, Reichenhainer Strasse 70, Chemnitz 09126, Germany

ARTICLE INFO

Keywords:
Human-robot collaboration
Speed and separation monitoring
Interference theory
Unstructured manufacturing

ABSTRACT

Human Robot Collaboration (HRC) has attracted high attention in modern manufacturing. Recently, a safety standard for collaborative robots has been launched (ISO/TS 15066). It cover the safety function of Speed and Separation Monitoring (SSM) which includes velocities and positions of the human and the robot. However, risk should be discussed with probability, while the SSM is not. Therefore, the probability of intrusion was calculated according to the stopping time of the robot and the maximum speed of the robot. Since the SSM was testified along the simulation by far, actual adhesive applying task was carried out in this paper.

1. Introduction

Industrial robots have been used for several decades and collaborative operation that enables collaboration between the humans and the robots has become increasingly of practical interest in the manufacturing industry [1]. Industrial robots, which have high precision in the manufacturing processes, can overcome the physical limitations of humans and perform risky tasks. However, it can be time consuming and inefficient to use industrial robots when the production is small. Furthermore, it is not easy to alter a process immediately to satisfy market needs. Therefore, it is difficult to use industrial robots in factories that produce products that require flexibility and complexity [2,3]. Consequently, human–robot collaboration (HRC) has been introduced to improve product quality and utilize a manufacturing layout where the robot carries out the simple and repetitive work while the worker operates on complicated assembly tasks [4].

For humans and robots to share work spaces, the safety integrity level of collaborative systems based on international safety standards [5,6] must be satisfied. The safety standard ISO/TS 15,066 ("Robots and robotic devices-collaborative robots") [7] describes safety functions to secure the safety of the workers. Speed and separation monitoring (SSM) is one of these functions that maintain sufficiently large distances to ensure safety by detecting the position and velocity of the human. Unlike other safety functions included in this standard, SSM allows mutual movement of the human and robot while ensuring that physical contact is avoided, helping robots and humans to work together. Therefore, by using SSM, sharing of workspaces can be expected [8] and the efficiency of production processes can also be improved.

Over the past few years, many researchers have shown an interest in the SSM method. In an early stage of the SSM development history, an evaluation mechanism for the SSM function was presented focusing on safety and productivity [9]. Further, an analysis of the current SSM function was reported based on simulation results [10]. In this study, the effect of the method measuring the speed of the robot on the SSM and the rationality of the elements constituting the SSM were studied and discussed. In another research, a likelihood analysis of the collaborative tasks based on tracking the human motion and the frequency of a cell in a space occupied by a human was carried out [11]. In addition, a dynamic SSM has been proposed, different from the existing calculation method of conventional safety distance, and its benefits and performance evaluation have been reported [12]. General safety factors, including SSM, were also investigated in terms of human presence sensing [13], collision avoidance [14–16], and danger fields [17].

Despite these efforts, the safety evaluation of the SSM function based on simulations has only been attempted for a two-dimensional analysis and has not been evaluated from the actual end-effector distance to the human. For this reason, the function of the SSM was likely to introduce or include an extra distance between the human and the robot. However, it is expected that the efficiency of the SSM will be increased by using a three-dimensional (3D) safety-related sensor. It is, therefore, important to investigate which of the parameters of the SSM function are sensitive to influence the safety distance with the growing

* Corresponding author.
E-mail address: kim.eugene@a.mbox.nagoya-u.ac.jp (E. Kim).
URL: http://www.mech.nagoya-u.ac.jp/asi/en/ (E. Kim).

https://doi.org/10.1016/j.rcim.2019.101819
Received 15 June 2018; Received in revised form 29 May 2019; Accepted 31 May 2019

increase in the use of 3D sensors [18,19]. The question remains how to quantitatively estimate the intrusion in the workspace in the designing stage of implementing SSM. In addition, the challenge lies to determine how to maintain work cell productivity without hampering the performance of the robot. Therefore, the present study was undertaken to examine the robot's performance and the effect of the environmental factors on the probability of intrusions in an actual collaboration scenario with a statistical interpretation.

In this study, a battery assembly task that includes an adhesive application by a robot was chosen as the collaborative task and implemented to measure the probability of human hand intrusion into the robot's protective separation distance (PSD). All tasks were based on HRC to investigate the probability of intrusion, and a statistical interpretation from interference theory (IT) was used for the analysis. Based on the actual HRC, we analyzed the tendency of intrusion probabilities into the PSD based on the stopping time and the parameters of the robot that supplement the PSD.

2. Speed and separation monitoring in human-robot collaboration

2.1. Protective separation distance

PSD is the smallest distance allowed between the human and the moving robot in a collaborative operation used by the SSM function. According to the ISO/TS 15,066 technical specification, when the separation distance, which is the distance between the human and the robot, decreases to a value below the PSD, a protective stop function should be executed immediately [20]. However, depending on the operation state of the robot, the speed and the inertia of the robot can vary on the basis of its payload or its pose and motion, which can increase the stopping distance. Therefore, it is necessary to maintain a safe distance between the robot and the worker to stop the robot, even when the operator cannot respond to the threat. Thus, PSD is expressed as the distance traveled by the human and the robot towards each other until the robot completely stops.

As shown in Fig. 1, assuming that the PSD $S_p(t)$ is a function of time t, the PSD at time t_0 can be expressed as follows:

$$S_p(t_0) = S_h + S_r + S_s + C + Z_d + Z_r, \tag{1}$$

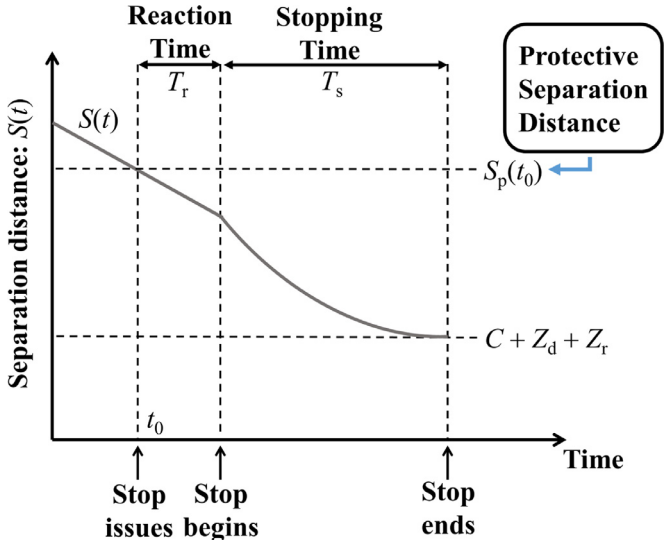

Fig. 1. Diagram of the safety function of Speed and Separation Monitoring. Protective Separation Distance consists of the minimum permissible distance between the robot and the human, S_h (distance that the human moves from stop issued until the robot stops), S_r (distance that the robot moves until it reacts), S_s (distance that the robot moves during braking), Intrusion distance C, and Uncertainties of measurement. Z_d and Z_r [7].

where S_h is the distance the human is expected to move from the time the stop signal is issued to the robot until the time taken by the robot to stop completely. Thus, in addition to the net time at which the robot must stop after receiving the stop signal, the additional reaction time, such as the time required for the communication between the safety-related sensor and the robot system, must be considered. S_r represents the reaction distance of the robot until the stop signal is issued by the safety-related sensors based on the human intrusion. It is assumed that the robot is moving with a constant speed until it receives the stop signal and reacts. The reaction time typically includes the response time of the safety-related equipment, the robot controller, and the communication latency. Furthermore, S_s is the distance that the robot travels from the time it receives the stop signal until it stops completely. Consequently, S_s is highly dependent on the stopping performance of the robot, the speed of the robot during the specific task, and the weight of the payload. In addition, C is an intrusion distance through which a part of the body (usually a hand) can move past the detected zone towards the hazard zone prior to actuation of the safety functions [21]. For example, safety sensors that monitor a two-dimensional plane, should consider the intrusion of the human body parts from the undetected intrusion, which can depend on the distance between the neighboring beams in case of a light curtain. Finally, Z_d and Z_r are the measurement uncertainties of the positions of the human and the robot, respectively. Z_d varies according to the performance of the safety-related sensor [22,23], and Z_r varies according to the accuracy of the robot's measurement system.

Furthermore, (1) can be written in more detail by substituting each term as follows:

$$S_p(t_0) = v_h(t_0)(T_r + T_s) + v_r(t_0)T_r + S_s + M. \tag{2}$$

It is assumed that T_r is the time elapsed from the moment the human enters the PSD until the robot reacts and T_s is the time elapsed from the issuing of the stop signal until the robot stops completely. Thus, the distance traveled by the human until the robot completely stops can be expressed as the product of the velocity of the human v_h at time t_0 and the sum of T_s and T_r. Next, the distance traveled by the robot until it responds is expressed as the product of the velocity v_r and T_r. Furthermore, the distance traveled until the robot completely stops can be predicted by integrating the speed v_s along T_s while the robot is decelerating.

$$S_s = \int_{t_0+T_r}^{t_0+T_r+T_s} v_s(t)\,dt. \tag{3}$$

Finally, the uncertainties in the measurements of Z_d, Z_r, and the intrusion distance C can be expressed to simplify to the equation using a margin factor M.

3. Human and robot interference theory

In HRC, human safety can be broadly classified into two types: psychological and physical safety [24]. Psychological safety refers to keeping the worker safe from threats such as mental fatigue or stress, which are constantly experienced in the work environment. Physical safety refers to keeping the operator safe from personal fatigue and injury from physical interactions of the robot with the worker. It is required to mitigate the risk to a tolerable limit through reasonable risk assessment and corresponding mitigation measures [25]. However, in this study, only physical safety is discussed to focus on the SSM functionality.

Physical safety can be interpreted as a guarantee of avoidance from unintended or unwanted contact between the human and the robot. Physical contact can occur only when the operator is at a distance close enough to collide with the robot and when the sensor system does not recognize the operator or the robot fails to stop. Therefore, in the process designing stage, it is important to know the probability of intrusion into the hazard zone based on the positions of the operator and

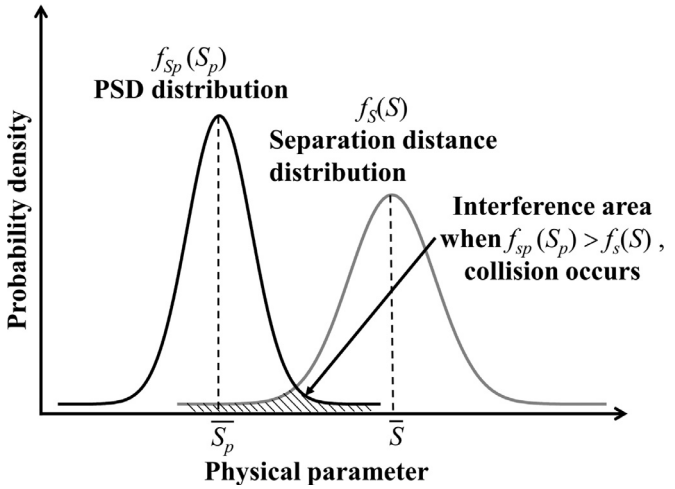

Fig. 2. Comparison of Protective Separation Distance S_p and the separation distance S distribution. Collision between the human and the robot can only occur when S is smaller than S_p. The distance is calculated along in direction of closest distance between the human and the robot.

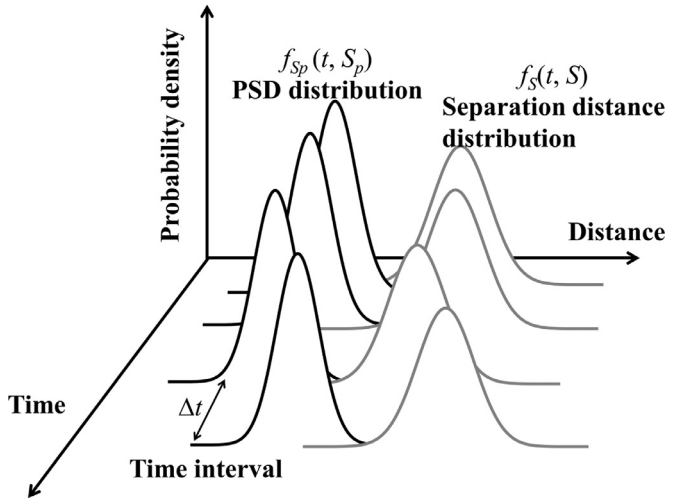

Fig. 3. Human and Robot Interference Theory comparing Protective Separation Distance and separation distance considering time variable. By considering the time variable when calculating the probability of intrusion, it is possible to prevent the probability of intrusion from being calculated excessively.

the robot. Herein, we propose the use of IT to investigate the probability of intrusion during the collaboration between the operator and the robot [26,27].

The concept of IT shows how the failure of the system can appear from a mechanical perspective [28]. By using IT, the PSD and the separation distance between the human and the robot are compared, as shown in Fig. 2. The projected area in Fig. 2 shows the portion of the interference between the two variables. When the distributions of the PSD and the closest distance are known, the general expression for the probability of intrusion can be written as

$$POI = P(S_p \geq S) = P(S_p - S \geq 0), \tag{4}$$

where POI is the probability of intrusion and each S_p and S represents a random variable of the PSD and separation distance, respectively. Therefore, a statistical expression of the POI using the PSD and closest distance can be rewritten as

$$POI = \int_{-\infty}^{\infty} f_{Sp}(S_p)\left[\int_{S_p}^{\infty} f_S(S)\,dS\right] dS_p, \tag{5}$$

where f_{S_p} and f_S are the probability density function of the PSD and the separation distance between the human and the robot, respectively. However, because both f_{S_p} and f_S terms are time dependent, if POI is calculated taking the time into account, the equation can be expressed as follows:

$$POI(t) = \int_{0}^{\infty} f_{Sp}(t, S_p)\left[\int_{S_p}^{\infty} f_S(t, S)\,dS\right] dS_p. \tag{6}$$

As shown in Fig. 3, by comparing the PSD and the separation distance including the time variable, it is possible to estimate the probability of intrusion in each time interval. In the analysis, because the domain of the PSD uses the physical parameter of the distance, only positive values were used in the integral domain. Note that POI is a function of t, and f_{Sp} and f_S are the probability density functions at a time interval $[t, t + \Delta t)$. Therefore, the POI can be defined by the time t and time interval Δt, and the POI for the total time T is expressed as follows:

$$\overline{POI} = \frac{1}{T}\int_{0}^{T}\int_{0}^{\infty} f_{Sp}(t, S_p)\left[\int_{S_p}^{\infty} f_S(t, S)\,dS\right] dS_p\,dt, \tag{7}$$

where $\overline{POI}$ denotes an averaged POI over the total time T.

To calculate $\overline{POI}$ more accurately, PSD must be calculated from the components of the velocities in the direction of the closest distance vector. As shown in Fig. 4, instead of using the velocity of the human v_h and the robot v_r, each of the velocities projected on the closest distance vector, v_h' and v_r', is used in the calculation. Furthermore, the maximum limit of the margin factor M in the calculation of the PSD (2) is assumed to be lower or equal to 850 mm [21], assuming that all 3D motions are detectable. In this study, only the collision between the end effector of the robot and the hand of the operator is considered as the most hazardous collision event. Therefore, the measured closest distance between the human hand and the end effector of the robot is used as the separation distance between the operator and the robot.

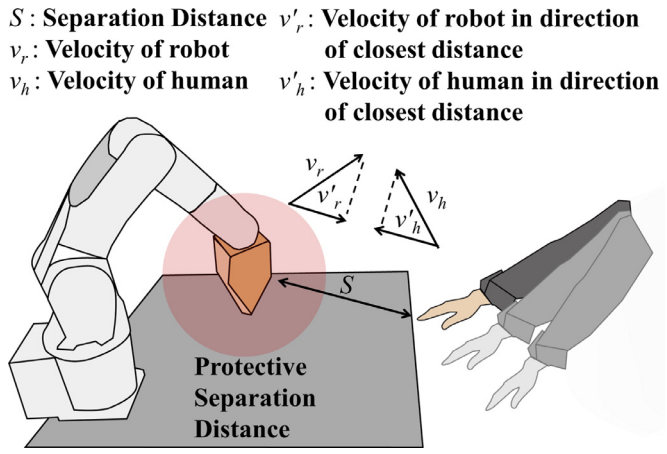

Fig. 4. The red sphere is the PSD that is calculated based on the velocity v_h of the operator's hand and the velocity v_r of the end effector of the robot particularly defined in direction of the closest distance from each other. Accordingly, the velocity v_h' of the worker's hand projected on closest distance vector and the projected velocity v_r' of the end effector of the robot is used in the calculation.

4. Experimental setups

4.1. Task setup

A battery assembling task was chosen to demonstrate the HRC task. An adhesive material must be applied to the corresponding battery junction in each direction to fix the battery cell into the case and the injection quantity should be adjusted by the proper amount. Therefore, the robot performed the adhesive application task and the battery-

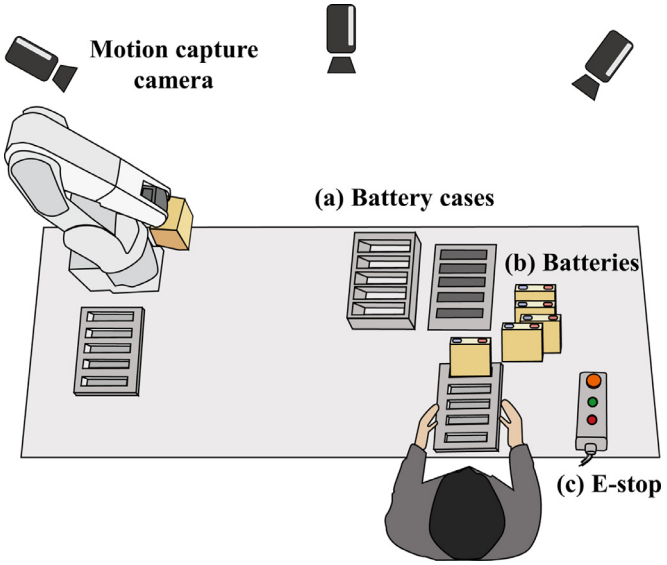

Fig. 5. Schematic diagram of human-robot collaboration work used in the experiment. The used battery assembly cooperative work is accomplished by combining (a) the battery case and (b) the battery cell. Here, the robot performs the work on the adhesive, and the E-stop is arranged within the workers reach.

Fig. 6. One of the participants doing the battery assembly work. Some of the layouts have been changed to make it easier to do the work for each of the participant and have improved the proficiency through several exercises.

assembling task was conducted by the human participant. Fig. 5 shows the schematic diagram of the experimental layout and Fig. 6 shows an actual image of the layout. However, only the application motion of the robot was demonstrated without actually using the adhesive. Next, to complete the task, a battery cell was inserted into each junction of the bottom case, and the battery case was assembled in the order of bottom, middle, and upper case.

- Battery assembly task:
  1. The operator installs the bottom case to the robot working space.
  2. The robot starts applying the adhesive to the bottom battery case.
  3. After the robot completes the operation, the operator installs the upper case in the robot's working space.
  4. The robot starts applying adhesive to the upper battery case.
  5. The operator inserts the battery cells into the bottom case during the upper case operation of the robot.
  6. The operator assembles the middle case.
  7. The operator assembles the upper case when the adhesive process of the upper case of the robot is completed.

4.2. Robot configuration and measurement setup

During the collaboration between the robot and the operator described above, it was assumed that the contact between the end effector of the robot and the hand of the operator was the most dangerous and was accompanied by the risk of injury. Therefore, the distance between the human and the robot was determined by measuring the distance of the hand (left or right hand) of the operator closest to the end effector of the robot. In this experiment, a motion capture system (Venus 3D), calibrated with a measurement error of less than 1 mm, was used to detect the movement of the robot end effector and the human hand in three dimensions with high accuracy. Seven cameras were used in the experiment, and the markers were attached to the tip of the end effector of the robot and both hands of the operator.

A six-axis robot arm, Denso VS-060, was used in the experiment and its maximum speed was set at 0.9 m/s. The stopping time of the robot was calculated based on the speed of the robot at every moment based on the data provided by the robot manufacturer. Based on the specification of the braking performance, stopping distance at every moment is calculated linearly from the instantaneous speed of the robot including the reaction time of the robot 0.1 s. The end effector was replaced by a soft urethane material, as unintended contact between the robot and the person that can occur during the experiment. In addition, to allow the operator to manually bring the robot to a safe state when desired, an emergency-stop button was placed close to the operator. Participants worked parallel to the robot at a distance of about 1.5 m from the center of the robot during the task so that the workers could not physically contact the robot, even if the workers reached out their hand. Ten healthy people participated in the experiment, and each participant assembled ten batteries.

5. Experimental results

5.1. Comparison of protective separation distance and separation distance

Fig. 7shows an example of the comparison of the calculated PSD and the separation distance using both the distance and the speed of the participant and the robot with respect to the world coordinate frame spanned at the motion capture system. The PSD was computed based on the relative speed of the robot and the operator. The intrusion distance C, which supplements the margin factor M, is the assumed distance required to detect human body parts successfully using the 3D safety-related sensor. No collisions between the human and the robot occurred

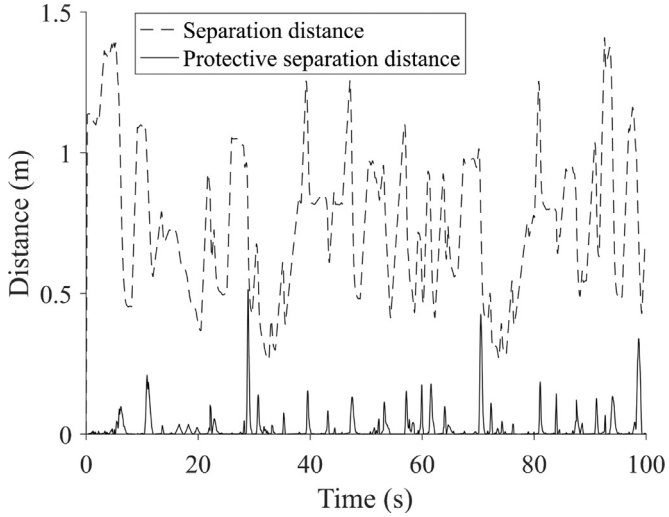

Fig. 7. Comparison of Protective Separation Distance (S_h, S_r and S_s only) and separation distance, which is derived by the actual speed and position of both the human hand and the robot end effector during experiment.

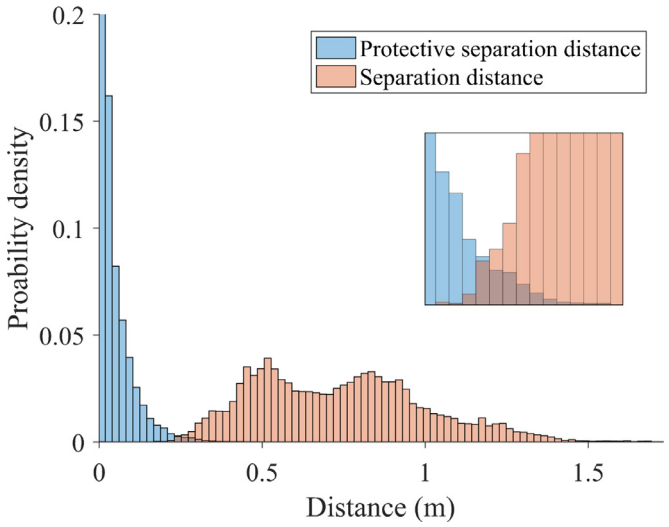

Fig. 8. Histogram of averaged distribution of closest distance between the operator and robot and the Protective Separation Distance of the ten participants until the task was completely over.

in this experiment.

As shown in Fig. 8, the PSD and the separation distance between the end effector of the robot and the separation distances of the ten people participating in the experiment were statistically compared. The average separation distance from the end effector of the robot to the operator was 0.74 m, and it required 7.5 min on an average to assemble ten batteries. Accordingly, the probability of the hand intrusion *POI* into the PSD using the IT in the battery assembly task was 1.2%.

In addition, Fig. 9 shows an example of the comparison between the PSD and the separation distance obtained by considering the time variable when setting the time interval Δt to 8 s. Consequently, the average $\overline{POI}$ for all of the ten participants was calculated to be 5.6×10^{-3}.

5.2. Simulation results of margin factor and stopping time in the probability of intrusion

As shown in the formula of PSD function (2), the calculation of the safety distance between the human and the robot comprises the margin factor *M*. Thus, the POI depends on the margin factor *M*, which is a

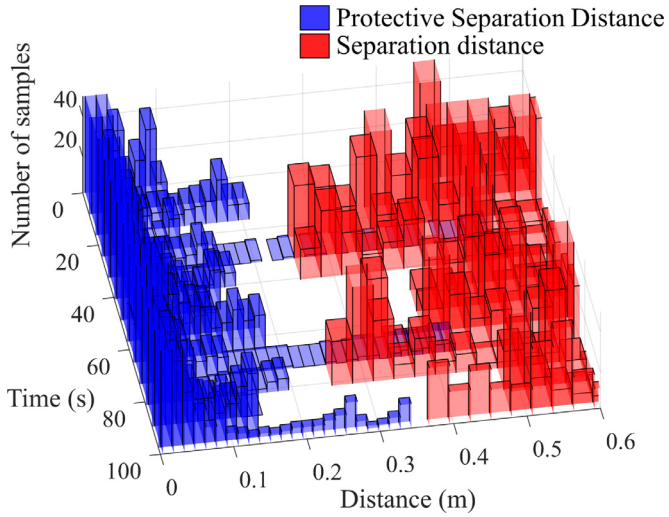

Fig. 9. Histogram of Protective Separation Distance and separation distance in each time period when the time interval is set 8 s.

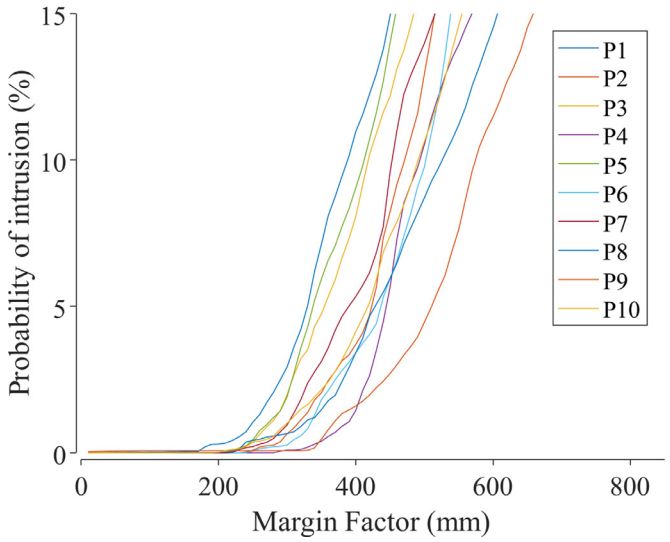

Fig. 10. Probability of intrusion into the Protective Separation Distance of ten participants in the experiment according to a margin factor *M*, which involves the intrusion distance *C* and uncertainties Z_d, Z_r. P1-P10 indicate the ten participants.

predetermined constant. Fig. 10 shows the simulation results of the $\overline{POI}$ in the PSD for each of the ten subjects when applying a different margin factor *M* in the PSD. The time interval Δt was set as 1 s, which includes 100 measured position samples of subjects and the robot. Accordingly, the probability of the human hand intrusion increased rapidly from 170 mm on an average, and over 1% of the intrusions were observed when a margin factor of 240 mm was applied. In addition, when using a margin factor greater than 650 mm, an intrusion probability of more than 15% was expected for the experimented task. By contrast, when excluding the margin factor, the probability of the human hand intrusion $\overline{POI}$ of all participants was 4.9×10^{-5}.

The stopping distance of the robot differs based on the robot inertia including the payload, robot pose, and velocity. Fig. 11 shows the simulation of the probabilities of the human hand intrusion into the PSD according to the different stopping time of the robot from the maximum

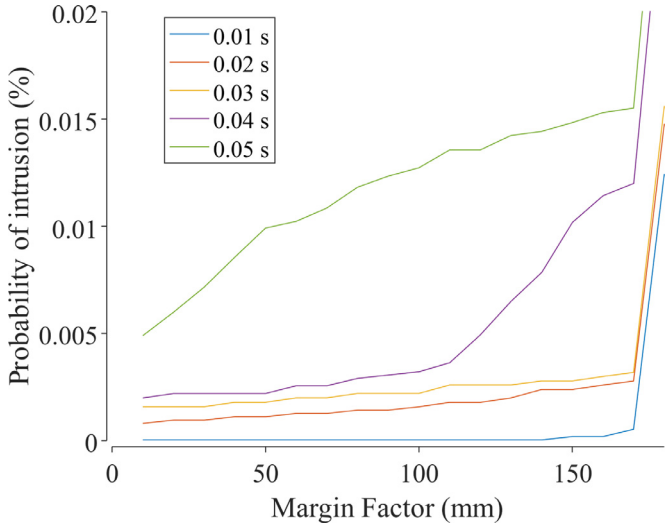

Fig. 11. Simulation of the probability of intrusion into the Protective Separation Distance using a robot with each stopping time according to the margin factor *M* when the maximum speed of the robot is 0.9 m/s. The stopping time is calculated linearly proportional to the instant speed of the robot. The greater the stopping time, the greater the probability of intrusion into the Protective Separation Distance.

Table 1
Calculation of PSD and POI using parameters of typical industrial robot parameters. The maximum velocity of a human was assumed to be 1.6 m/s and the reaction time of the robot was assumed as 0.1 s.

Physical parameters		Calculated results	
Stopping time (T_s)	Margin factor (M)	Maximum protective separation distance (S_{pmax})	$\overline{POI}$
0.05 s	850 mm	2.13 m	0.353
0.03 s	850 mm	1.72 m	0.352
0.01 s	850 mm	1.31 m	0.351
0.05 s	550 mm	1.83 m	0.175
0.05 s	350 mm	1.63 m	2.94×10^{-2}
0.05 s	150 mm	1.43 m	1.48×10^{-4}
0.05 s	10 mm	1.29 m	4.86×10^{-5}
0.03 s	550 mm	1.42 m	0.175
0.03 s	350 mm	1.22 m	2.70×10^{-2}
0.01 s	150 mm	0.61 m	1.55×10^{-6}
0.01 s	10 mm	0.47 m	0

speed T_s which affects the stopping distance of the robot S_s. Fig. 11 was generated with the average experimental data of the ten subjects. When the stopping time of the robot increased, the $\overline{POI}$ increased as well. Once the margin factor of 170 mm was exceeded a very rapid increase was observed. Finally, the simulation results based on the typical parameters of the stopping time and the margin factor are shown in Table 1.

6. Discussions

6.1. Application of speed and separation monitoring and limits

In comparison with the safety functions listed in ISO/TS 15066, SSM function has a strong advantage as it can enable HRC while using standard industrial robots [12]. For example, another collaborative principle, Power and Force Limiting, requires robots capable of detecting human contact. In addition, it is difficult to apply for tasks such as using heavy payloads or sharp tools where contact between the human and the robot is not allowed. In this respect, there is no doubt that SSM has a lot of potential in terms of application of collaborative work requiring non-contact and utilization of existing resources. However, robots designed with HRC in mind prefer the Power and Force Limiting function rather than the SSM function [10]. This may be because there are few safety-related sensors that can utilize the SSM functionality. Nevertheless, there are some constraints and application difficulties when implementing the SSM function.

One critical limit of the SSM is that each term in the PSD calculation is not easily defined, and it is difficult to choose the proper parameter values [10]. Although the explanations of the coefficients are provided in the ISO/TS 15066, the options to select the appropriate parameters specific to a situation depends heavily on the discretion of the safety integrator. Consequently, an evaluation method for each parameter must be provided subsequently and it is necessary to grasp the continuous technology trend for the SSM function to be applied with ease to all the robots.

For instance, the margin factor M in the PSD is subordinate to the workspace layout, which is not easily obtained specifically. The international standard, ISO 13,855 (”Safety of Machinery Positioning of Protective Equipment with Respect to the Approach Speeds of Parts of the Human Body”) [21], suggests guidelines for human physical parameters, especially including the choice of the intrusion distance C and maximum velocity of the human being. For example, the required intrusion distance C can be assumed as 850 mm maximum when the two-dimensional sensors cannot detect the human hand continuously. In this case, the robot should be separated by a distance greater than the intrusion distance C, and the worst-case distance the human can travel during the reaction time of the robot system. Moreover, the maximum velocity v_{hmax} of the human is assumed to be 1600 mm/s when the separation distance is greater than 500 mm and 2000 mm/s when it is lesser than 500 mm. However, the configuration of C can differ by the use of various safety measures including fences and safety doors.

Meanwhile, intrusion distance C can be diminished by detecting the intrusion of the hand by use of the 3D safety-related sensor making the HRC task faster and allowing the human and the robot to work in closer proximity. Furthermore, the workspace using the SSM function can be additionally configured and adjusted based on the probability of a human intrusion into the robot workspace. Specifically, even if the layout of the task process does not violate the SSM function and a small change in human behavior in actual collaboration causes a frequent halt of the robot, the layout of the workspace should be reorganized to meet the requirement of the safety regulation while maintaining the desired productivity in the process designing stage.

6.2. Probability of intrusion and practicality

The IT used in this study is a discrete statistical analysis method over time used to calculate the probability of intrusion. However, if the probability of intrusion is simply calculated for the entire collaborative work time, the characteristics of the partial intrusion tendency are ignored. Consequently, this creates difficulty in assessing how much of the interaction is involved in the detailed task and how much they cause intrusion. Conversely, if IT is used to calculate the probabilities of intrusion between the human and the robot, we can calculate how likely an intrusion is, in the local episodes between the time intervals of the intrusion distribution. For example, it is possible to predict how much the local probability of intrusion increases or decreases quantitatively as the number of tasks increases based on the data obtained during the work. This can limit or change the maximum speed of the robot to control the value of the probability of intrusion. In the process designing stage, it is possible to predict changes in the likelihood of an intrusion into the HRC system when the margin factors of the SSM function are changed. It is preferable that the arrangement of the tasks is set again if the robots are stopped frequently and the productivity is lowered, even though human presence detection is performed and the tasks are arranged by calculating the PSD using the SSM in the configuration step of the collaborative system. In addition, from an economic point of view, widening the distance between the robot and the human, reducing the speed of the robot, or reducing the payload could possibly reduce the probability of intrusion, which can bring about productivity benefits.

However, design of the time interval and the application of the POI also depends on the type of the collaborative task. If the task allows the human and the robot to interact continuously over a short distance, the time interval can be kept low to calculate the frequency with which the work was performed without violating the PSD. In this case, setting a larger time interval may lead to a higher POI than necessary. However, if the worker frequently needs to leave the collaborative space, or if the work is done in a large layout, it is more desirable to calculate the POI by generalizing the work time according to the categorized work, rather than using a constant time interval.

In this study, the POI was calculated with the distance between the human operator’s hand and the end effector of the robot, which has the widest moving range in general. However, in reality, not only the human hand but also any part of the upper or lower body or any part of the robot could be involved in a collision. For example, when an operator performs an operation of bending the upper body to inspect the product, the head of the operator is positioned closer to the robot than the hand. Similarly, each joint of the robot may collide with the body part of the worker. The estimation method using the IT proposed in this study can be improved by expanding the consideration to various human body parts. Therefore, to efficiently make use of the POI, 3D sensing technology is essential to the function of the SSM.

6.3. Influence of the margin factor and the stopping time on the probability of intrusion

The margin factor can be reduced by improving the performance of the safety-related sensor and increasing the measurable special dimension. This is because the measurement uncertainty can be reduced when the performance of the sensor device increases and the intrusion distance can be shortened when a 3-dimensional measurement is implemented. However, once the workspace is structured, the margin factor is likely fixed. Therefore, to construct the most efficient working environment it is important to know which variables are adjustable and which items are most effective to modify the margin factor.

During the simulation, reducing the margin factor and the stopping time can decrease the probability of intrusion. Increasing the margin factor, can be interpreted as reducing the distance between the human and the robot such that the difference between the PSD and an actual separation distance is reduced. Therefore, it can be seen that the probability of intrusion increases in the workspace of the robot when the distance between the human and the robot is slightly reduced through the simulation without actually changing the layout of the cooperative work.

With a high probability of intrusion, reducing the stopping time of the robot does not significantly decrease this tendency. This can be expected in the situation where the robot uses various tools, such as welding, drilling, moving, light, and heavy tools, and the change of the probability of intrusion based on the stopping speed caused by inertia difference. However, when the robot is light enough or does not use heavy tools, it is more effective to decrease the margin factor to reduce the probability of intrusion.

7. Conclusion

In this study, an experiment was conducted to investigate the Probability of Intrusion (POI) of a human hand into the Protective Separation Distance (PSD) in Human and Robot Collaboration (HRC) with the Speed and Separation Monitoring (SSM) function presented in the ISO/TS 15066. Throughout the presented experiment, Interference Theory (IT) was used to analyze the results, and its application for SSM-type applications was proposed. In particular, it was experimentally proven that if the time variable is considered in the IT, it is possible to prevent the POI of the human hand into the PSD from being overestimated.

In addition, to investigate the contribution of each component of the PSD to the POI of the human hand, a simulation based on typical parameters was executed. Consequently, it was shown that reducing the POI of the human hand is possible by modifying parameters such as the stopping time, the margin factors of the robot, and the safety-related sensor system, which represents the intrusion distance and the measurement uncertainties. Therefore, when using the SSM, the POI can be used as an index to validate the productivity while meeting the requirement of the safety regulation of the SSM based on the parameters that supplement to the PSD.

Conflict of interest

The authors declare no conflict of interest.

Acknowledgment

This study was conducted through “Knowledge Hub Aichi” project (Stage II - R6) which is financially supported by the Aichi Science and Technology Foundation.

References

[1] I. El Makrini, K. Merckaert, D. Lefeber, B. Vanderborght, Design of a collaborative architecture for human-robot assembly tasks, Intelligent Robots and Systems, 2017 IEEE/RSJ International Conference on, IEEE, 2017, pp. 1624–1629.
[2] A. De Meyer, J. Nakane, J.G. Miller, K. Ferdows, Flexibility: the next competitive battle the manufacturing futures survey, Strat. Manag. J. 10 (2) (1989) 135–144.
[3] A. Bauer, D. Wollherr, M. Buss, Human–robot collaboration: a survey, Int. J. Humanoid Rob. 5 (01) (2008) 47–66.
[4] J. Schlick, Cyber-physical systems in factory automation-towards the 4th industrial revolution, Factory Communication Systems (WFCS), 2012 9th IEEE International Workshop on, IEEE, 2012. 55–55
[5] Robots and Robotic Devices–Safety Requirements for Industrial Robots–Part 1: Robots, (2011). ISO 10218-1
[6] Robots and Robotic Devices–Safety Requirements for Industrial Robots–Part 2: Robot Systems and Integration, (2011). ISO 10218-2
[7] Robots and Robotic Devices–Collaborative Robots, (2015). ISO/TS 15066
[8] A.M. Zanchettin, N.M. Ceriani, P. Rocco, H. Ding, B. Matthias, Safety in human-robot collaborative manufacturing environments: metrics and control, IEEE Trans. Autom. Sci. Eng. 13 (2) (2016) 882–893.
[9] J.A. Marvel, Performance metrics of speed and separation monitoring in shared workspaces, IEEE Trans. Autom. Sci. Eng. 10 (2) (2013) 405–414.
[10] J.A. Marvel, R. Norcross, Implementing speed and separation monitoring in collaborative robot workcells, Robot. Comput. Integr. Manuf. 44 (2017) 144–155.
[11] A.R. Sanderud, M. Niitsuma, T. Thomessen, A likelihood analysis for a risk analysis for safe human robot collaboration, Emerging Technologies & Factory Automation (ETFA), 2015 IEEE 20th Conference on, IEEE, 2015, pp. 1–6.
[12] C. Byner, B. Matthias, H. Ding, Dynamic speed and separation monitoring for collaborative robot applications–concepts and performance, Robot. Comput. Integr. Manuf. 58 (2019) 239–252.
[13] D. Kulić, E. Croft, Pre-collision safety strategies for human-robot interaction, Auton. Robots 22 (2) (2007) 149–164.
[14] M. Chen, A.M. Zalzala, A genetic approach to the motion planning of redundant mobile manipulator systems considering safety and configurationJ. Robot. Syst. Banner(1995).
[15] S. Farsoni, F. Ferraguti, M. Bonfè, Safety-oriented robot payload identification using collision-free path planning and decoupling motions, Robot. Comput. Integr. Manuf. 59 (2019) 189–200.
[16] J.A. Marvel, R. Bostelman, A cross-domain survey of metrics for modelling and evaluating collisions, Int. J. Adv. Robot. Syst. 11 (9) (2014) 142.
[17] B. Lacevic, P. Rocco, Kinetostatic danger field-a novel safety assessment for human-robot interaction, Intelligent Robots and Systems, 2010 IEEE/RSJ International Conference on, IEEE, 2010, pp. 2169–2174.
[18] E. Kim, Y. Yamada, S. Okamoto, Improvement of safety integrity level by multiplexing radio wave sensors, System Integration, 2017 IEEE/SICE International Symposium on, IEEE, 2017, pp. 942–947.
[19] G.B. Avanzini, N.M. Ceriani, A.M. Zanchettin, P. Rocco, L. Bascettaf, Safety control of industrial robots based on a distributed distance sensor, IEEE Trans. Control Syst. Technol. 22 (6) (2014) 2127–2140.
[20] Safety of Machinery – Emergency Stop Function – Principles for Design, ISO 13850.
[21] Safety of Machinery – Positioning of Safeguards with Respect to the Approach Speeds of Parts of the Human Body, (2010). ISO 13855
[22] Safety of Machinery - Electro-Sensitive Protective Equipment - Safety-Related Sensors used for Protection of Person, IEC/TS 62998.
[23] Safety of Machinery - Electro-Sensitive Protective Equipment - Part 1: General Requirements and Tests, (2012). IEC 61469-1
[24] P.A. Lasota, T. Fong, J.A. Shah, et al., A survey of methods for safe human-robot interaction, Found. Trends® Robot. 5 (4) (2017) 261–349.
[25] Safety of Machinery – General Principles for Design – Risk Assessment and Risk Reduction, (2010). ISO 12100
[26] R.L. Disney, N. Sheth, C. Lipson, The determination of the probability of failure by stress/strength interference theory, Proceedings of the Annual Symposium on Reliability, (1968), pp. 417–422.
[27] K.C. Kapur, L.R. Lamberson, Reliability in Engineering Design, John Wiley and Sons, Inc., New York, 1977, p. 605.
[28] Z. Huang, Y. Jin, Extension of stress and strength interference theory for conceptual design-for-reliability, J. Mech. Des. 131 (7) (2009) 071001.